Environmental Research 305 (2026) 124994

Contents lists available at ScienceDirect

Environmental Research

journal homepage: www.elsevier.com/locate/envres

Contrasting spatial patterns of mercury and nitrogen in Mediterranean moss biomonitors: a multi-proxy survey across Tuscany (Italy)

Riccardo Fedeli [a], Kaylie Anne Walsh [a], Tiberio Fiaschi [a], Mirko Legnaro Diamanti [a], Stefano Loppi [a,b], Fabrizio Monaci [a,b,*]

[a] Department of Life Science, University of Siena, Via A. Mattioli 4, Siena, 53100, Italy
[b] National Biodiversity Future Center (NBFC), Palermo, 90133, Italy

ARTICLE INFO

Keywords:
Moss biomonitoring
Mercury
Nitrogen deposition
$\delta^{15}N$
$\delta^{13}C$
Mediterranean

ABSTRACT

Terrestrial mosses are widely used to monitor atmospheric deposition. However, concurrent assessment of mercury (Hg) and nitrogen (N), two pollutants characterized by different spatial scales of influence, from global to local, remains limited. To address this gap, we assessed Hg and stable isotopes ($\delta^{15}N$, $\delta^{13}C$) in pleurocarpous moss at 41 sites in Tuscany, central Italy. Concentrations of Hg ranged from 32 to 236 ng g^{-1} (median 64 ng g^{-1}) with a regional upper baseline of 95 ng g^{-1} (median + 2×MAD). Concentrations of Hg tended to decrease with distance from the Mt. Amiata cinnabar district ($\rho = -0.674$, $p < 0.001$) but showed no correlation with elevation, moss N content, or $\delta^{15}N$. In contrast, moss $\delta^{15}N$ (-4.16 ± 1.17‰) decreased significantly with altitude ($\rho = -0.369$, $p = 0.017$), consistent with attenuation of the lowland agricultural N-related signature at higher elevations. $\delta^{13}C$ values (-30.77 ± 1.20‰) increased with elevation ($\rho = +0.359$, $p = 0.021$), suggesting that C isotope discrimination in mosses may provide complementary information on site water-stress conditions. MixSIAR modelling indicated that atmospherically processed N (traffic NO_x and background wet deposition, considered jointly) accounted for almost the entire moss N budget, whereas the modelled contribution of direct agricultural NH_3 was negligible (<1%). The $\delta^{15}N$ signatures of these two processed pools are too similar to allow a reliable separation, so they are reported only as a combined term; this overall pattern remained stable across multiple sensitivity scenarios. Overall, the results of our study highlight the limitations of single-pollutant surveys in areas characterized by complex patterns of emissions and support the use of multiple proxies in biomonitoring.

1. Introduction

Human activities have profoundly altered global biogeochemical cycles through emissions of reactive nitrogen (N) and other atmospheric pollutants (e.g. sulphur compounds) that have had cascading effects on biodiversity, ecosystem functioning, and climate regulation (Fowler et al., 2013; Galloway et al., 2003, 2008; Galloway and Cowling, 2021). Despite the effectiveness of international conventions (e.g., the UNECE Gothenburg Protocol) to achieve substantial decline in sulphur and NO_x emissions across Europe, N deposition continues to be a concern particularly in southern Mediterranean regions which are not as well monitored (Izquieta-Rojano et al., 2025; Oenema et al., 2011). In addition to N, atmospheric deposition delivers multiple contaminants to the ecosystem. For instance, metals such as Cu, Pb, Ni, Cr or V can cause adverse effects on vital ecosystem functions, notably biological N_2 fixation in bryophytes (Scott et al., 2018), while Hg is taken up and accumulated by vegetation with a potential to biomagnify along food chains (Bargagli, 2016; Zhou et al., 2021). Thus, effective characterization of pollutant sources and their spatial distribution needs monitoring systems capable of detecting both deposition loads and regional emission fingerprints (Du et al., 2024; Petix et al., 2024).

Mosses are very commonly used as biomonitors of atmospheric deposition as they obtain nutrients from atmospheric inputs relying almost exclusively on wet and dry deposition (Bragazza et al., 2005; Du et al., 2022). Elemental composition and stable isotope ratios determined in pseudo-tissues of mosses allow for quantitative assessment of deposition and characterization of the sources (Díaz-Álvarez et al., 2018; Solga et al., 2006). Moss N correlates strongly with the total amount of N

This article is part of a special issue entitled: Biomonitoring environmental pollution published in Environmental Research.

* Corresponding author. Department of Life Science, University of Siena, Via A. Mattioli 4, Siena, 53100, Italy.
E-mail address: fabrizio.monaci@unisi.it (F. Monaci).

https://doi.org/10.1016/j.envres.2026.124994
Received 22 March 2026; Received in revised form 31 May 2026; Accepted 6 June 2026
Available online 8 June 2026

in atmospheric deposition (Du et al., 2022), while $\delta^{15}N$ signatures can effectively differentiate between reduced N forms (NH_x) from agriculture and livestock activities, typically with more negative $\delta^{15}N$ values. Fossil fuel combustion produces oxidized N forms (NO_x) that are typically reflected in less negative or positive $\delta^{15}N$ values (Bragazza et al., 2005; Felix et al., 2016; Izquieta-Rojano et al., 2025). Similarly, the $\delta^{13}C$ signature of mosses depends on the composition of CO_2 sources and on environmental conditions affecting carbon metabolism. Thus, this serves as an additional marker for anthropogenic CO_2 emissions and for ecological studies based on assessment of C3 or C4 photosynthetic pathway domination (Foan et al., 2014; Izquieta-Rojano et al., 2025).

In addition to being efficient monitors of atmospheric deposition, mosses, and more generally cryptogams, are considered major actors in Hg cycling within forest ecosystems. Indeed, global syntheses and field-based studies have demonstrated that vegetation uptake of gaseous elemental mercury (GEM, Hg^0) is the primary pathway of Hg deposition to terrestrial landscapes. Vegetation uptake is estimated to account for 60-90% of the Hg input to terrestrial ecosystems, and lichens and mosses generally have higher Hg concentration than vascular plants (Li et al., 2023; Obrist et al., 2021; Zhou et al., 2021). The spatial distribution of Hg is further complicated by altitudinal gradients. Mercury concentrations tend to be elevated in high-altitude cryptogams, even in areas remote from identifiable point sources. This enrichment is commonly decoupled with Hg in soil, suggesting an atmospheric origin for this Hg fraction attributed to the effect of “mountain trapping” (Shao et al., 2017) also known as “cold trapping” (Zeng et al., 2023). In Mediterranean ecosystems lichen and moss biomonitoring has revealed increased Hg and other trace elements deposition, associated with complex topography, slope aspect effects and exposure to regional wind (Bargagli, 2016; Bargagli et al., 2002; Vannini et al., 2021).

Combining $\delta^{15}N$ and $\delta^{13}C$ with conventional moss metrics (N and C contents, C/N ratios) has been shown to improve source attribution in recent continental-scale monitoring studies using moss as bioindicator of atmospheric deposition (e.g., Izquieta-Rojano et al., 2025). Indeed, the multi-pollutant capability of mosses and/or lichens used as biomonitors allows the simultaneous quantification of both Hg and N deposition indicators (Schröder et al., 2023), including $\delta^{15}N$ values that have been effectively used to discriminate N emission sources in Mediterranean environments (Barre et al., 2018; Izquieta-Rojano et al., 2016). However, vegetation uptake of GEM occurs through processes operating at fundamentally different spatial and temporal scales from those governing reactive N deposition, and the spatial coherence between Hg and N signals in moss biomonitors remains poorly investigated. Notably, surveys carried out at European scale have shown that Hg exhibits a relatively homogeneous spatial distribution, different from that of other metals and N (Harmens et al., 2015). This suggests that deposition pathways of these pollutants may diverge markedly in areas characterized by geogenic emissions (e.g., volcanic and hydrothermal Hg sources), volatilization of agricultural NH_3, NO_x emissions from traffic as well as orographic and coastal effects. Previous studies carried out in Tuscany, central Italy, have found strong correlations between moss N concentrations and modelled atmospheric N deposition (Jafarova et al., 2025) while the spatial distribution of Hg concentrations in mosses has been found to be influenced by altitude in a Tuscan mountainous area (Ancora et al., 2021). Therefore, assessing whether these elements in mosses co-vary spatially, or show independent distributions, has particular importance for the interpretation of biomonitoring data of trace and major elements and for understanding whether monitoring surveys based on a single pollutant or pollutant class can adequately capture total atmospheric deposition inputs.

The present study aimed to assess atmospheric Hg and N deposition across Tuscany on the basis of Hg concentration measurements and dual stable isotope analysis ($\delta^{15}N$ and $\delta^{13}C$) in terrestrial moss biomonitors at 41 sites. Specific aims of the research were to: (*i*) establish a regional baseline for moss Hg concentrations identifying spatial hotspots and influence at a regional scale of Mt. Amiata geogenic Hg anomaly, one of Europe's most significant geogenic Hg sources (McLagan et al., 2019); (*ii*) quantify the relative contributions of major N emission sources (agricultural NH_3, traffic NO_x, background wet deposition) using Bayesian isotope mixing models (MixSIAR) and (*iii*) assess spatial correlations, altitudinal gradients of elemental concentrations and isotopic values to test whether Hg and N signals in mosses eventually co-vary or differ spatially, thereby discriminating between coupled versus independent signals.

2. Materials and methods

2.1. Study area and sampling design

A total of 41 sampling areas were identified throughout Tuscany, central Italy (Fig. S1), taking into account the sampling design of the preliminary network of Jafarova et al. (2025; 33 sites) which was expanded to encompass the area of Mt. Amiata, characterized by a large geogenic Hg anomaly, and other areas potentially influenced by it in southern coastal Tuscany. The selection of the sites followed the protocol of the International Cooperative Programme (ICP) on Effects of Air Pollution on Natural Vegetation and Crops (ICP Vegetation, 2020), which recommends minimum distance rules in site selection: $\geq$300 m from main roads and villages, and $\geq$100 m from minor roads and buildings. Other protocol elements that were implemented in the study included the collection from undisturbed, open sites at least 3 m from the nearest projected tree canopy, the retention of only the green apical 3 cm of gametophyte shoots, and the pooling of five spatially independent sub-samples within a 50 m $\times$ 50 m plot into a single bulk sample. Where possible, the ICP protocol recommends collecting a minimum of 10 sub-samples; the lower density of the present study is consistent with previous Tuscan surveys (Jafarova et al., 2025) and was deemed adequate given the spatial homogeneity of moss cover at each plot and analytical sample-mass requirement for Hg and C-N isotope determinations.

At each site, moss samples were collected randomly. Since the same pleurocarpous moss species was not available for sampling at all sites, we adopted a multi-species approach, based on standard practice in European ICP monitoring surveys (Harmens et al., 2011, 2014). The restriction to pleurocarpous, carpet-forming taxa growing on undisturbed open ground was intended to constrain microhabitat conditions and gross shoot morphology, thereby limiting the larger trait contrasts that distinguish pleurocarps from acrocarpous or epiphytic mosses (Bargagli, 2016; Oishi and Hiura, 2017). To avoid any effect on the biomonitoring data from seasonal variability in atmospheric deposition, the samples were collected during a short period of time, approximately one week between 26 April and 3 May 2025. The potential impact of species differences on the measured variables (Hg, N%, C%, $\delta^{15}N$, $\delta^{13}C$) and the derived C/N ratio was assessed using the Mann-Whitney *U* test comparing the data for *Hypnum cupressiforme* (the most represented species, 33% of sites) against the remaining pleurocarpous species pooled. Median values did not differ significantly between the two groups (all $p > 0.05$) and the effect sizes were small (all $|r| < 0.25$, Table S1), suggesting that species identity is unlikely to account for the regional patterns reported in the present study. This comparison should, however, be regarded as a screening-level test, since pooling the less frequent taxa into a single group precludes the detection of effects specific to individual species.

2.2. Sample preparation

In the laboratory, moss samples were cleaned of extraneous material (litter, soil particles and invertebrates) with plastic tweezers under a stereo-microscope. To ensure temporal comparability of deposition signals across species with differing whole-shoot longevity (Harmens et al., 2011) only green, actively growing tissue from the apical 3 cm of gametophyte shoots, corresponding to the last 2-3 years of growth,

was retained for the analysis. Samples were then oven-dried at 40 °C to constant weight and ground to powder using a ceramic mortar and pestle (Legnaro Diamanti et al., 2026). Homogeneous subsamples were assigned for Hg and C, N, $\delta^{15}N$ and $\delta^{13}C$ analysis.

2.3. Mercury analysis

The total mercury in the moss tissues was determined with a Direct Mercury Analyzer (DMA-80, Milestone S.r.l., Italy) according to USEPA Method 7473. Dried, homogenized material (10-30 mg) was weighed into nickel boats and thermally decomposed, amalgamated, and the Hg content determined at 253.7 nm by atomic absorption spectrophotometry. A calibration curve in the range 0.5-100 ng mL^{-1} of Hg standards was prepared from a 1000 mg L^{-1} Merck Hg standard solution. Analytical quality control measures consisted in the analysis of procedural blanks, duplicates and certified reference materials (e.g. NIST SRM 1515 Apple Leaves; Finnish Forest Research Institute SRM M2; Steinnes et al., 1997) which showed recoveries in the range 95-105%. The limit of detection (LOD) was 0.5 ng g^{-1} dry weight.

2.4. Carbon, nitrogen and stable isotopes

Total nitrogen (N %) and carbon (C %) contents and $\delta^{15}N$ and $\delta^{13}C$ isotopic compositions were measured via an elemental analyzer-isotope ratio mass spectrometer (EA-IRMS; Delta Q coupled to an IsoLink CN interface; Thermo Fisher Scientific) at the EASIER (Elemental and Stable Isotope Ecology Research) facility of the National Biodiversity Future Center (University of Siena, Italy). About 2 mg dry moss were weighed into tin cups and combusted in the Elemental Analyzer. The produced gases (N_2, CO_2) were chromatographically isolated and introduced into the IRMS in a continuous-flow mode.

Isotopic compositions are expressed in δ notation (‰) relative to international standards which were atmospheric N_2 for $\delta^{15}N$ and Vienna Pee Dee Belemnite (VPDB) for $\delta^{13}C$. Analytical precision from repeated measurement of internal standards (acetanilide, caffeine) and International Atomic Energy Agency reference materials (IAEA-600, IAEA-41a and USGS54), was ±0.15‰ for $\delta^{15}N$ and ±0.10‰ for $\delta^{13}C$. Blanks and laboratory controls were run in each batch to validate measurement accuracy.

2.5. Data analysis

All statistical analyses were performed in R (version 4.3.2; R Core Team, 2025). The variables were summarized using descriptive statistics, and normality was assessed by the Shapiro-Wilk test. Because concentrations of Hg were not normally distributed, the Spearman's rank coefficient (ρ) was used to investigate correlations among chemical parameters and between isotopic ratios and elemental concentrations. Regional backgrounds were identified as median +2×MAD (Median Absolute Deviation) which is a highly robust method (Reimann et al., 2005). We defined regional Hg baseline values on the basis of a three independent-method triangulation technique (robust statistics, median +2×MAD; percentile (p90); Empirical Cumulative Distribution Function (ECDF) breakpoint identification). By adopting this multi-method approach, we achieved statistical robustness with respect to non-normal distributions, which is common in geochemical data (Reimann et al., 2005).

For quantifying the relative contributions of atmospheric N sources to moss tissues we used the Bayesian isotope mixing model based on MixSIAR (Stock and Semmens, 2016). For maximum comparability and representativeness, we implemented the methodology used by Izquieta-Rojano et al. (2025) for attributing the N source in mosses from 15 European countries, to obtain quantitative estimates of source proportions from the isotopic mass balance equation:

$$\delta^{15}N_{mixture} = \Sigma\left(p_i \times \delta^{15}N_i\right)$$

where p_i is the proportional contribution of source i (constrained to $\Sigma p_i = 1$), and $\delta^{15}N_i$ is the isotopic signature of that source. The model was defined by three end-members representing the major atmospheric N pools reported in European biomonitoring surveys (Harmens et al., 2011; Izquieta-Rojano et al., 2025): 1) Agricultural NH_3 from livestock volatilization and fertilizer application ($\delta^{15}N = -28.0 \pm 11.0$‰, mean ± SD, n = 17; Du et al., 2024); 2) Traffic NO_x from vehicular combustion emissions ($\delta^{15}N = -7.3 \pm 7.8$‰, n = 151; Du et al., 2024), and 3) Background wet deposition, representing regional processed NH_4^+ deposited via precipitation ($\delta^{15}N = -6.42 \pm 4.4$‰, n = 200; Ciężka et al., 2016; Xu et al., 2019).

We did not apply any isotopic fractionation correction to the data (Bragazza et al., 2005; Dawson et al., 2002), since ^{15}N discrimination during N assimilation by bryophytes is minimal (<0.5‰; Bragazza et al., 2005). To determine posterior distributions without imposing assumptions about source dominance, ensuring comparability with Izquieta-Rojano et al. (2025), our model used non-informative priors (uniform Dirichlet distribution, $\alpha = 1$ for all sources). Markov Chain Monte Carlo (MCMC) with three chains ("very long" protocol) of 1,000,000 iterations each (500,000 burn-in, thinning = 500; Stock and Semmens, 2016) was used to sample posterior distributions. As recommended by Gelman and Rubin (1992), convergence diagnostics confirmed adequate mixing (all R-hat <1.01) while sensitivity analyses with alternative prior specification allowed us to verify model robustness. We recognize that, according to the indication of Phillips et al. (2014), a single isotopic tracer can resolve at most two sources in a mixing framework and the near-identical mean $\delta^{15}N$ values of Traffic NO_x and Background wet deposition ($\Delta = 0.9$‰) limit the model's capacity to resolve these two pools and to interpret their posterior estimates. Nevertheless, a three-source configuration was chosen for this study as we wanted to ensure the direct comparability with MixSIAR assessment conducted at continental scale by Izquieta-Rojano et al. (2025), who applied the same end-member definitions across 1311 sites in 15 European countries.

Point and interpolated maps were created with QGIS. Spatial patterns of Hg concentrations in Tuscan mosses were visualized by ordinary kriging using the SAGA backend; Hg data were interpolated on UTM-projected sampling points using a 100 m output grid, 100 lag classes, automatic maximum lag distance and were fitted to a linear variogram model ($a + b \times h$) without logarithmic transformation or block kriging. Due to the limited number of sites (n = 41) and the uneven spatial density across the region, no cross-validation, variogram residual analysis or uncertainty mapping was performed. Therefore, the kriged surface is intended as visual aid to the reader and does not imply predictive or geostatistically validated interpolation.

3. Results and discussion

3.1. Elemental and isotopic composition of moss tissues

Total Hg concentrations showed marked spatial variability, ranging between 31.5 and 235.6 ng g^{-1} (Table 1). This right-skewed distribution (Shapiro-Wilk $W = 0.817$, $p < 0.001$) reflects the presence of sites with

Table 1
Descriptive statistics of Hg, N and C concentrations, C/N ratios and $\delta^{15}N$ and $\delta^{13}C$ in pleurocarpous mosses collected from 41 sites across Tuscany, central Italy (April - May 2025).

Parameter	Mean	SD	Median	Min	Max	P90
Hg (ng g^{-1})	78.9	44.4	63.7	31.5	235.6	129.0
N (%)	1.26	0.32	1.22	0.63	2.45	1.54
C (%)	42.1	4.3	42.9	22.2	51.4	44.4
C/N	34.9	7.8	33.5	17.9	56.4	44.2
$\delta^{15}N$ (‰)	−4.16	1.17	−4.39	−6.83	−1.63	−2.54
$\delta^{13}C$ (‰)	−30.77	1.20	−30.73	−34.59	−28.48	−29.36

anomalously elevated Hg concentrations (Fig. 1). Overall, Hg concentrations in this study were comparable with those recorded in other moss surveys conducted in Europe (Harmens et al., 2015). Our data also agree with ranges reported by Bargagli (2016) for *H. cupressiforme* from Tuscan areas impacted by geothermal activities, except for Hg concentrations measured at hotspots, such as sites near geothermal power plants.

Nitrogen content varied considerably across the 41 sites (0.63-2.45%, mean 1.26 ± 0.32%), in line with the data recently published for surveys in many countries in Europe (mean ± SD: 1.27 ± 0.45%; range 0.40 - 3.95%) by Izquieta-Rojano et al. (2025) and comparable to the Tuscan regional value of 1.15 ± 0.42% reported by Jafarova et al. (2025) for a 2021 field campaign that included 33 of the 41 sites of the present study. Notably, our spatial variability in N content (CV = 25.4%) is lower than that reported by Jafarova et al. (2025; CV = 36.5%), probably because of the extended geographic coverage of our monitoring network, which captured more remote, high-altitude areas. From the comparison of our data with the classification of the ICP European moss surveys (Harmens et al., 2011, 2014) atmospheric N deposition in Tuscany was quite moderate, ranging from environments characterized by low deposition (<0.8%, such as those of northern Finland and northern UK) to hotspots (>1.6%, such as central Germany, Belgium, and parts of Slovenia).

The C content of our mosses was rather steady (42.1 ± 4.3%) and was accompanied by C/N ratios varying between 17.9 and 56.4 (mean ± SD: 34.9 ± 7.8), a range about 8% lower than the corresponding value of 38.1 reported by Izquieta-Rojano et al. (2025) for 15 European countries. This difference may reflect species-specific metabolic differences, though site-to-site heterogeneity can be considerable. As expected, we also found a strong negative association between N% and C/N ratio ($\rho = -0.935$, $p < 0.001$) which supports the expected response of C, which remains relatively homeostatic through photosynthetic regulation, whereas N accumulation responds directly to atmospheric deposition with minimal internal buffering (Bragazza et al., 2005), which makes this parameter a good indicator of potentially enhanced atmospheric N inputs (Du et al., 2022; Izquieta-Rojano et al., 2025).

Values of $\delta^{15}N$ in the moss samples of this study were consistently depleted with respect to atmospheric N_2 and ranged between −6.83 and −1.63‰. The mean (±SD) of the Tuscan mosses (−4.16 ± 1.17‰) well matched the European value of −4.85‰ (range −10.35 to +6.60‰; Izquieta-Rojano et al., 2025); however, we refrain from performing a meaningful regional comparison with the Italian $\delta^{15}N$ values of −5.62 ± 0.83‰ (n = 20) reported by Izquieta-Rojano et al. (2025), as the geographic distribution of the Italian sites is not specified in their publication. Consistent with this interpretation, 80.5% of our samples (33/41) had $\delta^{15}N$ values < −3‰, which is a typical threshold for regimes dominated by ammonia (Díaz-Álvarez et al., 2018; Zhao et al., 2019); moreover, at all our sites $\delta^{15}N$ values were always lower than 0‰, suggesting no or limited influence from traffic NO_x, which is commonly indicated in moss by less negative or positive $\delta^{15}N$ values (Donovan et al., 2022; Felix et al., 2016; Izquieta-Rojano et al., 2025). This distribution pattern suggests a widespread influence of reduced N (NH_x) related signatures in Tuscany, consistent with the presence of a regional agricultural matrix dominated by olive and vineyard cultivation and by non-intensive livestock farms, potentially releasing NH_3 from manure and fertilizers, that may influence the N budget. At eight sites (19.5%) transitional signatures (−3 to 0‰) were observed, possibly indicating a mixture between the on-site agricultural ammonia and combustion-derived NO_x emissions.

The variability of $\delta^{13}C$ was considerably smaller (mean ± SD: −30.77 ± 1.20‰; range −34.59 to −28.48‰) and fell within typical ranges for the C3 photosynthetic pathway of bryophytes and for the

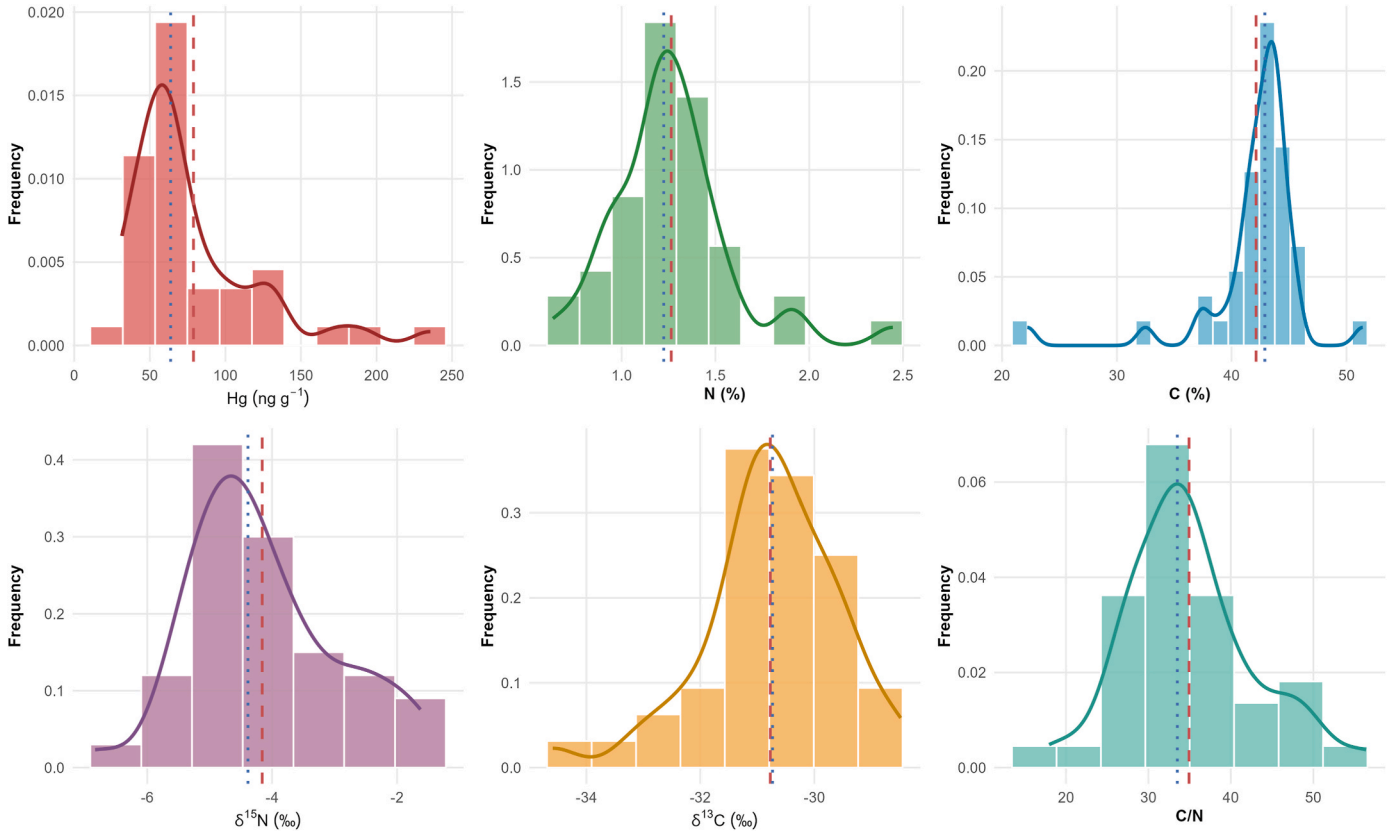

Fig. 1. Frequency distributions of Hg (ng g^{-1}), N (%) and C (%) concentrations, N ($\delta^{15}N$, ‰) and C isotopic ratios ($\delta^{13}C$, ‰), and C-to-N ratios (C/N) measured in moss collected from 41 sites. Respective mean (red dashed lines) and medians (black dotted lines) are reported in each graph. (For interpretation of the references to colour in this figure legend, the reader is referred to the Web version of this article.)

reported Mediterranean moss values (−32 to −28‰; Izquieta-Rojano et al., 2025). Tuscan samples are slightly higher than the European average of −31.60‰, a pattern that persists across all regional $\delta^{15}N$ ranges, probably resulting from response to water stress regulation under Mediterranean drought period (Bramley-Alves et al., 2015; Skrzypek et al., 2007) and/or potential contribution of ^{13}C-enriched soil dust at arid sites (Bargagli et al., 1995; Izquieta-Rojano et al., 2016). In bryophytes under desiccation, intracellular CO_2 concentrations decrease and photosynthetic activities are reduced. As a consequence, CO_2 diffusivity through water film on the surface of cells also decreases, resulting in less negative $\delta^{13}C$ signatures of plants growing under water-limited conditions (Deane-Coe et al., 2015). Since site-specific meteorological information is not available in our study as well as in many other moss surveys, mechanistic interpretations of $\delta^{13}C$ variation remain speculative, and caution in this regard has been recommended when using the stable isotope methods in biomonitoring projects (e.g. Izquieta-Rojano et al., 2025). The spatial distribution of $\delta^{15}N$ and $\delta^{13}C$ values across the sampling network is shown in Fig. S2.

3.2. Mercury baseline and spatial distribution: the Mt. Amiata geogenic influence

Inspection of the ECDF graph (Fig. 2a) identified a natural breakpoint at 73.0 ng g^{-1} (coinciding with the 66th percentile) as the maximal local value that lies below the elevated tail. Following Reimann et al. (2005), cumulative probability plots of these inflection points can be suggestive of changes in geochemical populations. Baseline in Hg concentration in Tuscan moss was identified at a threshold of 95.0 ng g^{-1} (median + 2×MAD; Reimann et al., 2005). High Hg accumulation observed at 10 local sites (representing 24.4% of the monitoring sites) was above this level. The four sites with the highest Hg concentrations (hotspots; 133-236 ng g^{-1}) exceeded the 90th percentile (129.0 ng g^{-1}; Fig. 2a).

No significant correlation was found between Hg concentrations in moss and altitude across the elevation gradient of the sampled sites (27-1580 m a.s.l.; $\rho = -0.231$, $p = 0.146$, Fig. 2b). This result contrasts with biomonitoring studies from remote montane areas around the world that documented significant positive relationships between altitude and Hg concentrations in mosses. For instance, in a study conducted on the Tibetan Plateau, the strong positive correlations with altitude ($r = +0.362$, $p < 0.05$) in mosses and lichens were attributed by Shao et al. (2017) to the "mountain cold trapping" effect that enhanced atmospheric scavenging of Hg at high elevations. Notably, Ancora et al. (2021) reported, specifically for Mt. Amiata, higher accumulation of Hg in mosses and lichens at high elevation, suggesting this altitudinal effect is best observed within a single mountain. However, at the scale of a regional monitoring network including multiple mountain systems and sources, like in Tuscany, local-scale trapping signals appear to be diluted, yielding weak or no relationships with altitude (e.g., Cai et al., 2024; Sonke et al., 2023). In our study, the regional geogenic/anthropogenic Hg flux creates a horizontal distance-decay gradient ($\rho = -0.674$, $p < 0.001$ for Hg vs. distance from Mt. Amiata) that may override any vertical atmospheric gradient, resulting in concentrations 2-4 times the regional median (63.7 ng g^{-1}) within the anomaly zone (<50 km from the geogenic source) regardless of elevation (Fig. 2b). This zone is well represented by a geographical pattern of Hg concentration following clear SW-NE gradient across Tuscany (Fig. 3). Localities over the breakpoint value of 73.0 ng g^{-1} are mostly located in the SW part, correlating with the regional metallogenic context, such as Site 23 (Monte Argentario, 236 ng g^{-1}), Site 20 (Talamone, 191 ng g^{-1}), Site 38 (Alberese, 171 ng g^{-1}) and Site 31 (Sovana, 133 ng g^{-1}). This spatial coherence of statistical outliers with known geogenic anomalies confirms that the ECDF breakpoint approach is indeed a valid one for the differentiation between background and anomalous Hg enrichments (Fig. 3).

In southern Tuscany, a large area including the Colline Metallifere and Mt. Amiata is distinguished by polymetallic mineralization (Hg, As, Sb and base metals) associated with Neogene magmatism and hydrothermal activity (Lattanzi, 1999; Monaci and Baroni, 2025 and references therein). Mt. Amiata is among the largest Hg districts in the world. Here, passive air sampling documented time-weighted gaseous Hg concentrations ranging from background levels (1.5-2 ng m^{-3}) to > 6000 ng m^{-3} near abandoned mining facilities (McLagan et al., 2019). In the past, also several geothermal power plants contributed to Hg recirculation in the area, but recently they have been equipped with modern abatement systems that have substantially reduced these

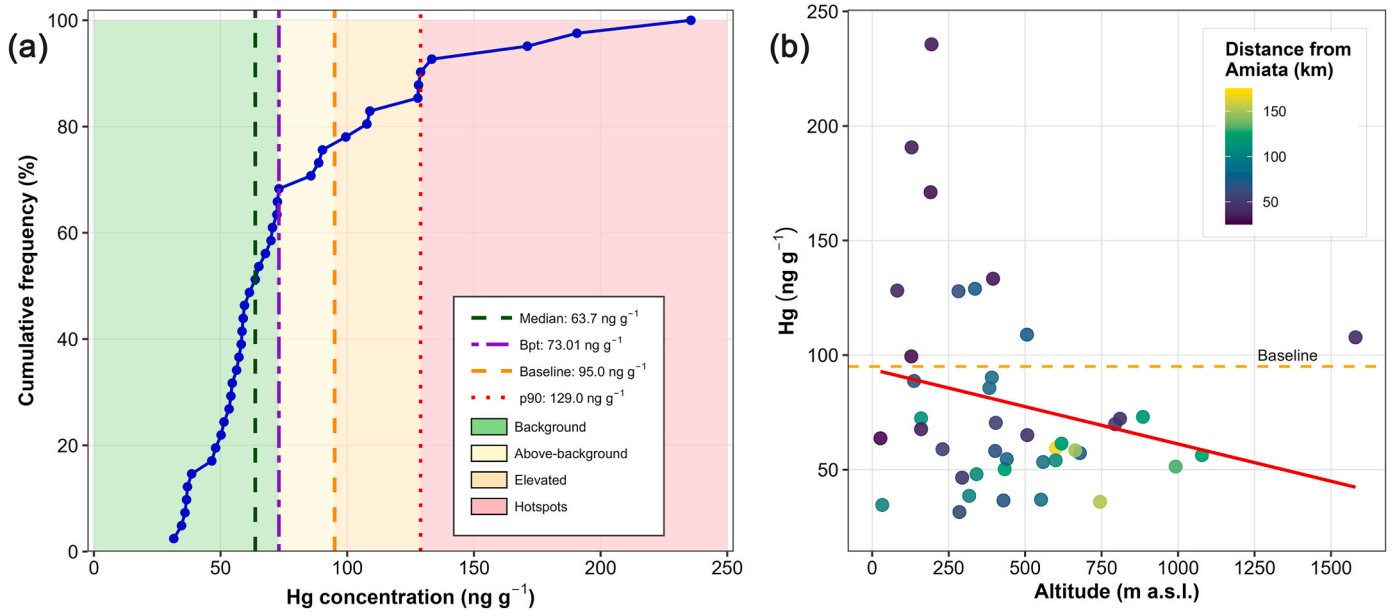

Fig. 2. Distribution and altitudinal patterns of Hg concentrations in Tuscan mosses (n = 41). (a) ECDF and baseline thresholds (Reimann et al., 2005): background (63%), above-background (20%), elevated (10%), hotspots (7%). Bpt.: breakpoint; p90: 90th percentile. (b) Hg versus altitude coloured by distance from Mt. Amiata. Linear regression (red line): $\rho = -0.231$, $p = 0.146$. (For interpretation of the references to colour in this figure legend, the reader is referred to the Web version of this article.)

Fig. 3. Hg concentrations (ng g^{-1}) in moss tissues at 41 sites in Tuscany (see Fig. S1 for site locations and identifiers) with interpolated Hg layer created with ordinary kriging shown as semi-transparent blended overlay using a continuous colour ramp scaled by quantiles. The Tuscan Archipelago islands were not included in the monitoring network and were therefore excluded from the spatial interpolation. The Florence conurbation and the main geochemical anomaly areas (Colline Metallifere, Mt. Amiata) are shown. Basemap imagery: Regional boundary and geographic layers of SIPT Regione Toscana - Geographic Information System. (For interpretation of the references to colour in this figure legend, the reader is referred to the Web version of this article.)

emissions (Monaci et al., 2023).

The high Hg concentrations found in mosses on the southern coast deserve special attention. The maximum recorded value (236 ng g^{-1}, Site 23) was found on the Monte Argentario promontory, a carbonate headland located on the Tyrrhenian Sea coast of southern Tuscany and connected to the mainland by two Holocene tomboli, Giannella and Feniglia. The promontory is characterized by Calcare Cavernoso (Upper Triassic) outcrops with Fe-Mn oxides and polymetallic sulfides mineralizations (Protano et al., 2023), which represent a geogenic source of Hg consistent with the anomalous moss concentrations recorded at this site. Pasquetti et al. (2020) showed that Late Pleistocene sediments of the nearby Ansedonia coastal plain are characterized by pre-industrial Hg enrichments (0.2–2.7 mg kg^{-1}) deriving from geogenic sources. Hg levels in the Quaternary continental deposits of this zone are up to 4.55 mg kg^{-1} with maximum value of 14.9 mg kg^{-1} in samples collected at a depth of 6 m whereas the stream sediments from watercourses draining the coastal plain present concentrations included between 0.97 and 3.8 mg kg^{-1} (Protano et al., 2023 and references therein). These geochemical anomalies, ascribable to regional Hg sources which outcrop in the Mt. Amiata district and local sedimentary processes, indicate that the southwestern Tuscan coast lies within a region characterised by Hg enrichment where natural Hg sources are more important than anthropogenic inputs. The higher concentration of Hg in moss at Sites 20 and 38 (Fig. S1), located in the Monti dell'Uccellina sector, is indicative of cinnabar mineralization related to the Mesozoic limestones of this zone. The excavation of cinnabar deposits dating back to the Late Neolithic (ca. 4490–4330 cal BC; Poggiali et al., 2017) provides further support to this long-term geogenic nature of the Hg anomaly in this portion of the coast.

Based on the estimates made by Li et al. (2023) in the subtropical montane forest ecosystems of Southwest China, uptake of GEM accounts for approximately 90% of total Hg accumulated in mosses. In Mediterranean environments like those of southern Tuscany, and especially in the Mt. Amiata area, the contribution of wet and particle-bound Hg could be relevant and Hg enrichment of moss tissues from local re-emission and inputs from soil resuspension cannot be excluded. Consistent with this interpretation, the differences observed in this study between background sites (mean: 58 ng g^{-1}) and hotspots (133-236 ng g^{-1}) appear to reflect the enrichment of Hg^0 above the hemispheric baseline that occurs in the southern part of the region (Fig. 3), with the coastal gradient indicating variable contributions from longer-range transport and localized geogenic inputs.

3.3. Spatial independence of Hg and N signals in moss

No significant correlations were observed between $\delta^{15}N$ and Hg ($\rho = 0.035$, $p = 0.829$) or between Hg and N% ($\rho = 0.283$, $p = 0.073$), suggesting that at the regional scale both Hg and reactive N deposition are largely governed by independent spatial drivers (Fig. 4). This independence was maintained after accounting for altitude, as partial correlations remained typically non-significant even when the ten hotspot sites (Hg > 95 ng g^{-1}) were excluded (filtered Hg ≤ 95:$\rho = 0.229$, $p = 0.215$ for Hg vs N%; $\rho = -0.137$, $p = 0.461$ for Hg vs $\delta^{15}N$; Fig. 4a–b); thus confounding by geogenic outliers on the correlation structure can be ruled out. The negative correlation of N% and C/N ratio ($\rho = -0.935$, $p < 0.001$; Fig. 4d) confirmed the internal reliability of the N deposition signal, which is consistent with an observed accumulation of atmospheric N in moss tissues without much internal buffering (Bragazza et al., 2005; Du et al., 2022).

Overall, the different responses of Hg and $\delta^{15}N$ to altitude provided consistent evidence that Hg and reactive N signals respond to different spatial drivers. Our data show a negative correlation between the $\delta^{15}N$ values in mosses and altitude ($\rho = -0.369$, $p = 0.017$; Fig. 5a), consistent with the agricultural NH_x emissions primarily occurring at lower altitudes and their dilution by background atmospheric N as the elevation increases. This altitudinal trend contrasts with that found in the Austrian moss surveys (Zechmeister et al., 2008), where $\delta^{15}N$ in moss tissues was found to increase with altitude in response to enhanced dry and occult (fog/cloud) deposition occurring in Alpine environments. The divergent trend we obtained in mosses of Tuscany can probably be attributed to the unique features of this Mediterranean region, where agricultural activities, rarely intensive, occur essentially in the lowland plains while upland sites are located far from direct NH_x source emissions. In addition, the relatively modest altitudinal range of our study (<1580 m a.s.l.) must also be considered with respect to studies where positive trends were reported (spanning gradients up to > 2500 m a.s.l.; Oishi, 2019; Zechmeister et al., 2008). Atmospheric N deposition in high-altitude Alpine environments is dominated by particulate NH_4^+ and NO_3^- and other chemical species from long-range transport and/or characterized by regional admixture which commonly carry isotopically enriched ^{15}N signatures relative to local gaseous NH_x sources (Balestrini et al., 2024). Therefore, the altitudinal range sampled in the present study does not appear to be such as to cause this shift in deposition regime, and the $\delta^{15}N$ gradient is instead governed by the horizontal distribution of agricultural emissions across the Tuscan landscape. A survey conducted in a similar Mediterranean setting in Portugal documented a dominant NH_x influence at the regional scale which was attributed to intensive agriculture causing the most depleted $\delta^{15}N$ values in lichen biomonitors (Pinho et al., 2017). Other studies, across Europe, have documented negative associations between $\delta^{15}N$ and the inputs from intensively farmed areas or from high atmospheric NH_3 concentrations (Boltersdorf et al., 2014; Izquieta-Rojano et al., 2025).

The positive correlation of $\delta^{13}C$ with altitude ($\rho = +0.359$, $p = 0.021$) shown in Fig. 5b also confirms the altitudinal patterns in isotopic signatures observed in Tuscan mosses. In fact, the increase in $\delta^{13}C$ values as elevation increases is consistent with the role of water availability in controlling C isotope discrimination since drought conditions at higher elevations were found to result in less negative $\delta^{13}C$ values in moss tissue because of the reduced water film thickness on cell surfaces, limiting CO_2 diffusion (Bramley-Alves et al., 2015). A similar pattern was observed along a European latitudinal gradient with the mosses showing the most enriched $\delta^{13}C$ values in southern Mediterranean regions where hydric stress was more pronounced. However, the authors of this study (Izquieta-Rojano et al., 2025) cautioned about the possibility that site-specific environmental factors could also have an impact on moss $\delta^{13}C$ spatial distribution.

As non-vascular plants lacking a true root system and a protective cuticle, mosses absorb water and solutes directly from atmospheric inputs across the entire shoot surface (Bargagli, 2016). Their Hg signal

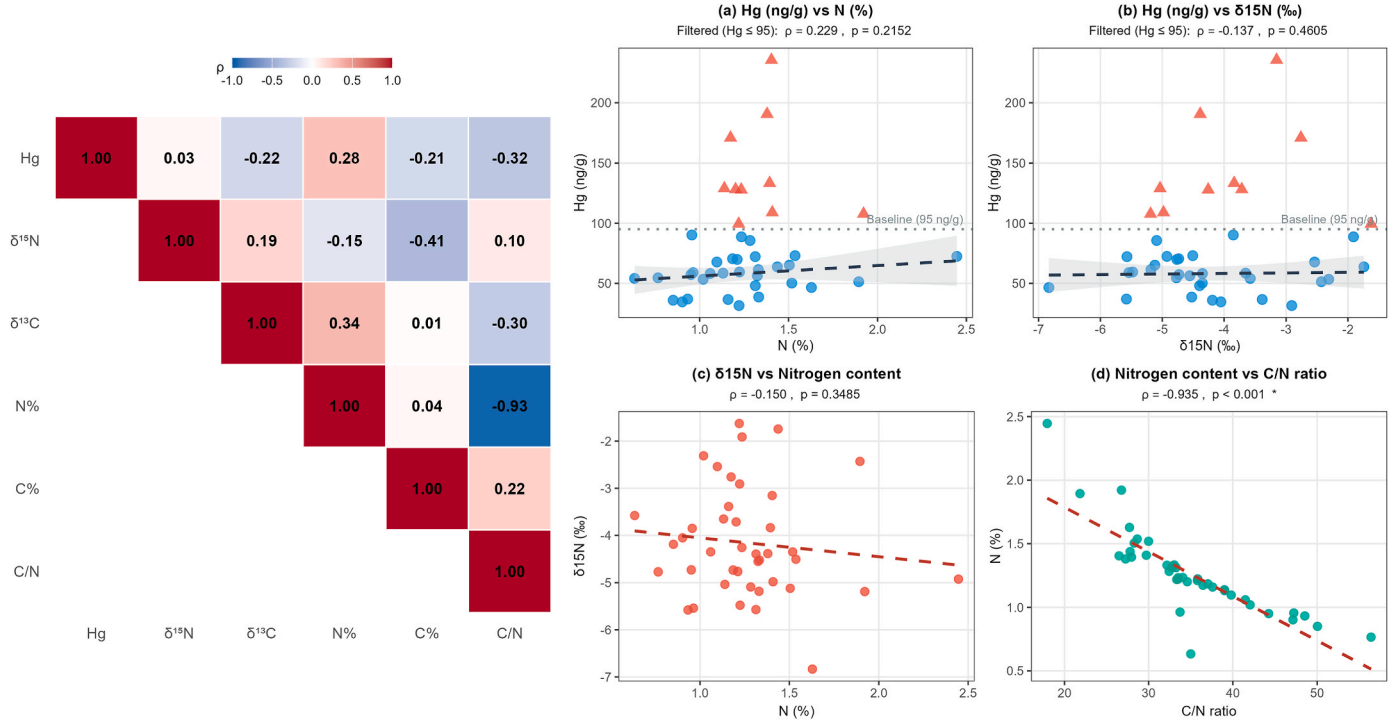

Fig. 4. Correlation matrix and bivariate relationship between elemental and isotopic parameters in moss samples (n = 41). On the left, heatmap showing pairwise correlation coefficients among Hg, $\delta^{15}N$, $\delta^{13}C$, N%, C%, and C/N ratio. On the right, scatterplots showing (a) the correlation between Hg and N%, (b) Hg vs $\delta^{15}N$, (c) $\delta^{15}N$ vs N%, and (d) N% against C/N ratio. In panels (a) and (b), blue dots indicate sites below baseline (Hg ≤ 95 ng g^{-1}, n = 31), red triangles values above baseline (n = 10) while regression lines with 95% CI are on filtered data only. (For interpretation of the references to colour in this figure legend, the reader is referred to the Web version of this article.)

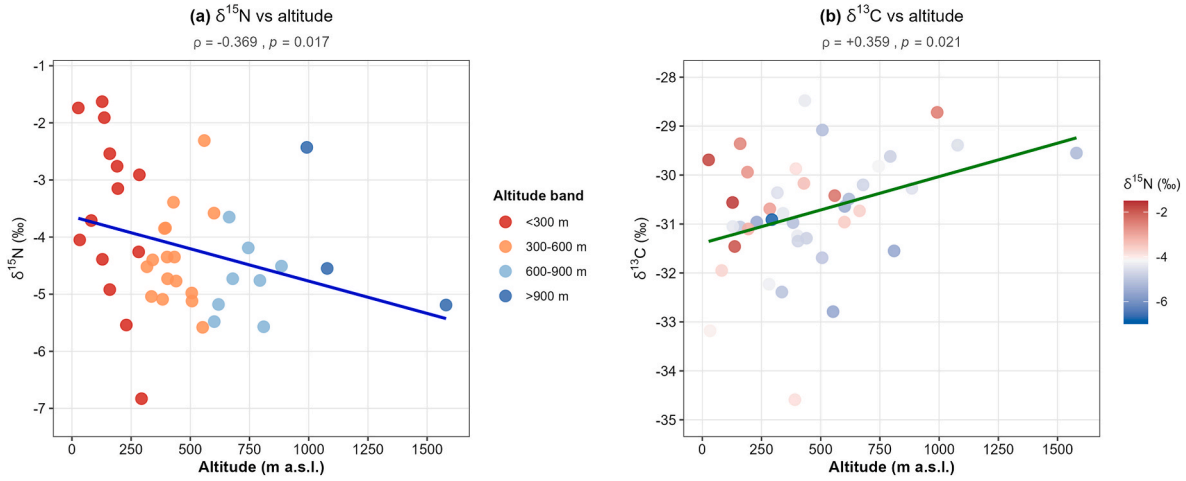

Fig. 5. Altitudinal gradients of stable isotope signatures in moss samples from Tuscany (n = 41). (a) $\delta^{15}N$, coloured according to altitude band; and (b) $\delta^{13}C$, coloured according to value of $\delta^{15}N$. Linear regression lines, Spearman (ρ) correlation coefficients are indicated.

therefore integrates multiple deposition pathways operating simultaneously rather than reflecting a single dominant flux. The different spatial responses of Hg and N in moss are consistent with their specific drivers at the regional scale. In forested areas without strong local sources, dry deposition of GEM is generally considered the dominant pathway among the mechanisms controlling Hg uptake from the atmosphere (Li et al., 2023; Obrist et al., 2021); however, mosses may also take up Hg delivered by wet deposition of oxidized mercury species (Hg^{2+}) and by particle-bound Hg (Bargagli, 2016). In geogenically anomalous areas such as Mt. Amiata, contributions from locally re-emitted and soil-derived Hg cannot be excluded, given the strong point-source emissions documented for the area (McLagan et al., 2019).

Disentangling these co-occurring pathways based on concentration data alone remains difficult. A recent isotope survey in an alpine coniferous forest (Xu et al., 2026) quantified this partition in both terricolous mosses and epiphytic lichens, and demonstrated that in these remote environments atmospheric Hg(II) represents a large proportion of the Hg pool in cryptogams ranging from about 51% in ground-dwelling moss mats of *Actinothuidium hookeri* to 27% for mosses (*H. plumaeforme*) at the base of the trunk, with epiphytic lichens characterized by a similar range (31-52%). In addition, the same study highlighted that species identity and ecophysiological factors such as thallus morphology and tissue longevity together modulate Hg accumulation. As a consequence, concentration surveys like ours can map spatial patterns of Hg accumulation but cannot fully resolve the relative importance of deposition pathways or species-specific differences. Multi-isotope end-member models built on $\Delta^{199}Hg$, $\Delta^{200}Hg$ and $\delta^{202}Hg$ are the most straightforward way to clarify both gaps and applying this framework to the Mt. Amiata geogenic gradient would be the natural methodological continuation of the present work.

The contrasting spatial behaviour of Hg and N documented here is likely to extend beyond Tuscany. In fact, these dynamics can likely occur in other Mediterranean and semi-arid regions where natural Hg anomalies spatially interact with N emissions from traffic or agriculture. The Mediterranean basin has several terrestrial landscapes which are well-known for being enriched by Hg, such as the Iberian Pyrite Belt, the geothermal Aegean volcanic arc and Campanian volcanic fields (Bargagli, 2016). In these areas, source complexity can severely limit the applicability of moss biomonitoring due to multiple deposition pathways of different chemical species. In such contexts, a multi-proxy framework, like that of this study, combining elemental and stable isotope analysis with Bayesian source apportionment and with the support of a standardized biomonitoring protocol, may represent a useful transferable approach.

3.4. Nitrogen source apportionment

Bayesian posterior estimates are reported in Table 2 and Fig. 6. The model estimated agricultural NH_3 contribution at less than 1% of moss N (posterior mean 0.7%, 95% CI: 0.0-2.6%), whereas Traffic NO_x and background wet deposition combined were estimated to account for nearly the entire moss N budget (posterior means of 21.4%, 95% CI: 3.5–40.8%, and 77.9%, 95% CI: 58.4–95.6%, respectively). The internal partitioning between these two processed pools should be regarded only as indicative since they differ in mean $\delta^{15}N$ by only 0.9‰ and this relatively slight isotopic offset, together with the intermediate values of the Tuscan moss mean ($\delta^{15}N = -4.16 \pm 1.17$‰) between both end-members, limits the possibility of discrimination of any model. This limitation is well-documented when source signatures approach analytical precision (Phillips et al., 2014; Stock et al., 2018) and it is also shared by the seven-source model of Izquieta-Rojano et al. (2025) used for a continental-scale assessment, which also relied on $\delta^{15}N$ as the sole tracer.

We tested four MixSIAR configurations based on different end-members, priors and data subsets all of which showed agricultural NH_3 contributed less than 2.1% of reactive N and the upper 95% credible interval was 5.8% (see Supplementary Material Section S1 and Table S2 for full details). Across the four sensitivity scenarios, the estimated contribution of primary agricultural NH_3 remained negligible and was not substantially altered by the choice of end-members, priors or

Table 2
Bayesian isotope mixing model results for nitrogen source apportionment in Tuscan mosses (n = 41).

N Source	$\delta^{15}N$ End-Member (‰)[a]	Mean Contribution (%)	95% Credible Interval[b]	Reference
Agricultural NH_3	−28.0 ± 11.0	0.7	0.0-2.6	Du et al. (2024)
Traffic NO_x	−7.3 ± 7.8	21.4	3.5-40.8	
Background wet deposition	−6.42 ± 4.4	77.9	58.4-95.6	Xu et al. (2019); Ciężka et al. (2016)

[a] End-member isotopic signatures represent source emissions (mean ± SD) compiled from European-scale literature syntheses. [b] Posterior estimates derived from MCMC sampling. Wide credible intervals reflect partial isotopic overlap between Traffic NO_x and Background wet deposition end-members ($\Delta^{15}N = 0.9$‰), limiting model discriminatory power (Phillips et al., 2014).

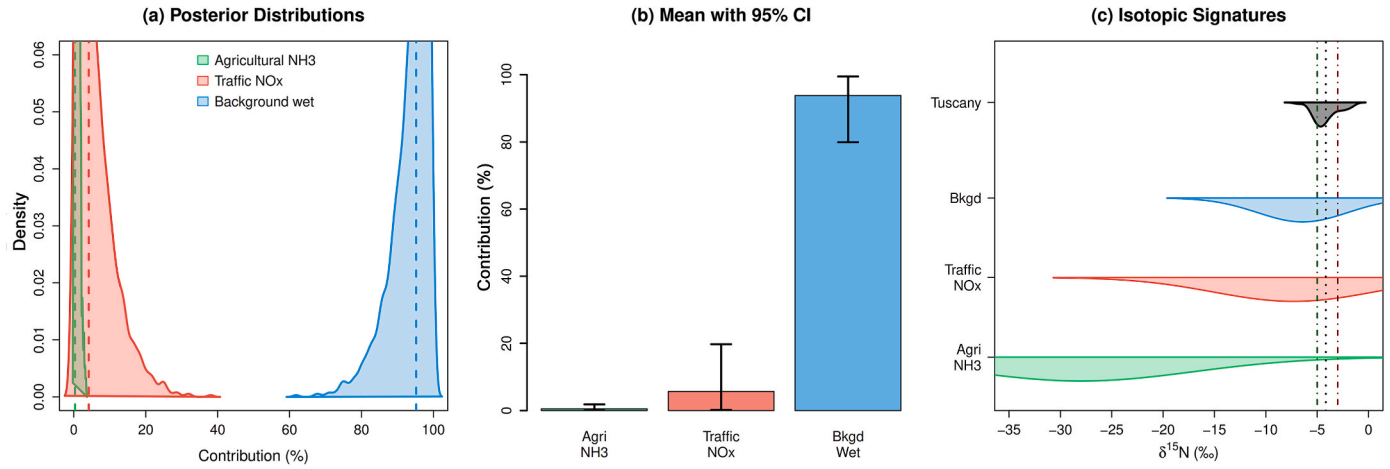

Fig. 6. Nitrogen source distribution by Bayesian mixing model (MixSIAR). (a) Posterior probability distributions for each source obtained from MCMC sampling (dashed lines = medians of posterior). (b) Average source contributions along with 95% credible intervals (error bars). (c) End-member source isotopic composition (coloured distributions) in comparison with Tuscan moss mixture (gray). Vertical dashed lines at $\delta^{15}N = -5‰$ and $-3‰$ represent the levels of agricultural NH_3 and traffic NO_x, respectively (Felix et al., 2016; Xiao et al., 2010). Moss mean (−4.16‰, dotted line) lies between overlapping sources and accounts for posterior uncertainty.

data subset. In addition, the dominance of atmospherically processed N (traffic NO_x + wet deposition combined: ca. 99%) in the present study aligns well with the results reported by Izquieta-Rojano et al. (2025). Applying a qualitative threshold-based classification process (Felix et al., 2016; Xiao et al., 2010), 24.4% of the sites had $\delta^{15}N$ values lower than −5‰, indicative of substantial influence from NH_3. On the other hand, 19.5% of the sites showed that $\delta^{15}N$ site values were larger than −3‰, a threshold that therefore indicates NO_x sources. At first glance, these site frequencies might suggest a stronger agricultural influence than the <1% calculated by the MixSIAR model. The two approaches are, however, fundamentally different: the threshold classification is site-specific and yields qualitative indicators of source dominance, whereas the Bayesian mixing model produces region-wide, quantitative estimates of source contributions for each of the 41 sites across the study area (Stock and Semmens, 2016).

In our interpretation of the results, the low contribution we obtained for primary agricultural NH_3 emissions to Bayesian posterior estimates does not exclude agricultural N impacts as it could be related to the fast atmospheric conversion of gaseous NH_3 to particulate (NH_4^+) through reaction with acidic species (Sutton et al., 1993), and the subsequent incorporation of NH_4^+ in background wet deposition. Once mixed into this pool, NH_4^+ loses its original source marker and is effectively accounted for by the mixing model within the background wet deposition term, rather than as primary agricultural NH_3. In addition, NO_x from vehicular traffic is photochemically oxidized to nitrate (Seinfeld and Pandis, 2016), leading to regional wet deposition. Therefore, the isotopic signal characteristic of sites directly influenced by local agricultural emissions may be overprinted at the regional scale by broader atmospheric N inputs that are mainly marked by isotopically aged deposition (Heaton et al., 1997). Long-range transport may further contribute to this signal (Fowler et al., 2013). This interpretation is consistent with the sampling protocol we used (ICP Vegetation, 2020) which specifies that monitoring sites must be located farther than 300 m from main roads and beyond 100 m from clear agricultural point sources. As a consequence, it is not surprising that our study mostly reflects diffuse, regionally mixed atmospheric inputs rather than specific local emissions.

Our MixSIAR results are in line with the European moss survey conducted by Izquieta-Rojano et al. (2025), a survey including 1311 sites from 15 countries, mostly from central and northern Europe, that reported wet deposition ($NH_4^+ + NO_3^-$) contributing 31-51% to moss N while gaseous uptake (primary $NH_3 + NO_x$) accounted for 38-52%. In our study we found a greater proportion for wet deposition, reaching 77.9% with respect to the European mean (around 43%). This may be mainly attributable to climatic characteristics since, differently to the more evenly distributed wet deposition regimes of northern Europe, in Mediterranean areas episodic, high-intensity precipitation events may act as efficient scavenging process of atmospheric N species (Lovreškov et al., 2021). Moreover, our Tuscan monitoring network (41 sites covering 22,990 km^2) has a relatively low site density with respect to agricultural hotspot regions in Belgium or the Netherlands (Harmens et al., 2015) and this may result in undersampling of localized agricultural influence, with a bias of the regional estimate toward background sources.

For Tuscany, we estimated a contribution of NO_x traffic of 21.4%. This datum falls within the European range of 10-51%, very variable among countries, commonly reaching the highest values in densely urbanized regions like Belgium (55% from combustion sources) and the lowest values where rural landscapes are predominant (Izquieta-Rojano et al., 2025). This intermediate position of Tuscany in the European range probably reflects the mixed land use mosaic of the region in which extensive agricultural plains (Val di Chiana, Maremma) are intersected by road networks (Autostrada A1, regional highways) that connect main urban areas and are surrounded by vast montane forests where atmospheric mixing is likely to homogenize source signals (Jafarova et al., 2025).

4. Conclusions

In the present study, we provide a first integrated assessment of atmospheric Hg and N deposition patterns in a Mediterranean region by measuring Hg concentrations alongside dual stable isotope analysis ($\delta^{15}N$, $\delta^{13}C$) in terrestrial moss biomonitors, across 41 sites in Tuscany.

Key findings of our study indicate that the spatial distribution of Hg was largely driven by the geogenic hotspot of Mt. Amiata, highlighted by a strong and significant distance-decay gradient and the occurrence of hot spots (133-236 ng g^{-1}) which were 1.4 to 2.5 times the regional baseline (95 ng g^{-1}). The lack of an Hg-altitude relationship suggests that, especially in the southern part of the region, the horizontal geogenic gradient is strong enough to mask any vertical atmospheric trapping effects commonly documented in remote mountain systems.

Nitrogen isotopic signatures reflected the spatial distribution of agricultural emissions, with more depleted $\delta^{15}N$ values at lower elevations where NH_x sources are concentrated (agricultural NH_3 in the

lowland). Bayesian isotope mixing models indicated that atmospherically processed N (wet deposition and traffic NO_x combined) accounted for nearly the entire moss N budget, whereas the modelled contribution of direct agricultural NH_3 inputs was negligible. The internal partitioning between wet deposition and traffic NO_x should be considered as indicative rather than quantitative, due to the near-identical isotopic signatures of these two end-members ($\Delta^{15}N = 0.9‰$; Phillips et al., 2014) and this is consistent with the rapid atmospheric processing of primary NH_3 and NO_x emissions prior to deposition at remote sites.

Taken together, our results indicated spatially distinct patterns for Hg and N, consistent with the hypothesis that the atmospheric processes governing their accumulation in mosses operate largely independently at the regional scale. On this basis, Hg in Tuscan mosses appears more strongly influenced by geogenically driven gradients, whereas N isotopic signatures appear to track the regional distribution of agriculture and combustion emissions across the landscape. This spatial independence persisted after the exclusion of outliers and after controlling for altitude, indicating that the pattern was not substantially altered by these factors.

These findings point to three directions for future biomonitoring work. First, Hg, N and isotopic measurements could be integrated into the sampling framework of future ICP Vegetation campaigns to identify pollutant interactions that are relevant to ecosystem risk assessment. Second, the conventional sampling protocol could be complemented by targeted sampling transects in regions of known geogenic Hg anomalies, preferentially based on a single moss species where the target taxon is consistently available, to minimise interspecific variability in Hg, N and C signals, with the aim of characterizing spatial gradients and mapping the spatial extent of geogenic influence. Finally, Hg stable isotope analysis based on mass-independent ($\Delta^{199}Hg$) and mass-dependent fractionation ($\delta^{202}Hg$) could be applied to samples collected along such transects. Although applications at regional scale of this approach to moss biomonitoring are relatively scarce, such analyses could support source apportionment at the air-vegetation interface and help link deposition trends to indicators of ecosystem health.

Funding

This work was supported by the National Recovery and Resilience Plan (NRRP), project “National Biodiversity Future Center - NBFC” (CN_00000033, CUP B63C22000650007).

CRediT authorship contribution statement

Riccardo Fedeli: Conceptualization, Investigation, Writing – original draft, Writing – review & editing. **Kaylie Anne Walsh:** Data curation, Investigation, Writing – review & editing. **Tiberio Fiaschi:** Investigation. **Mirko Legnaro Diamanti:** Investigation. **Stefano Loppi:** Conceptualization, Resources, Writing – review & editing. **Fabrizio Monaci:** Conceptualization, Data curation, Formal analysis, Funding acquisition, Software, Visualization, Writing – original draft, Writing – review & editing.

Declaration of competing interest

The authors declare that they have no known competing financial interests or personal relationships that could have appeared to influence the work reported in this paper.

Acknowledgments

Fabrizio Monaci and Stefano Loppi were supported under the National Recovery and Resilience Plan (NRRP), Mission 4 Component 2 Investment 1.4 - Call for tender No. 3138 of 16 December 2021, rectified by Decree n.3175 of 18 December 2021 of Italian Ministry of University and Research funded by the European Union - NextGenerationEU; Award Number: Project code CN_00000033, Concession Decree No. 1034 of 17 June 2022 adopted by the Italian Ministry of University and Re-search, CUPB63C22000650007, Project title “National Biodiversity Future Center - NBFC”.

Appendix A. Supplementary data

Supplementary data to this article can be found online at https://doi.org/10.1016/j.envres.2026.124994.

Data availability

Data will be made available on request.

References

Ancora, S., Dei, R., Rota, E., Mariotti, G., Bianchi, N., Bargagli, R., 2021. Altitudinal variation of trace elements deposition in forest ecosystems along the NW side of mt. Amiata (central Italy): evidence from topsoil, mosses and epiphytic lichens. Atmos. Pollut. Res. 12, 101200. https://doi.org/10.1016/j.apr.2021.101200.

Balestrini, R., Diémoz, H., Freppaz, M., Delconte, C.A., Caschetto, M., Matiatos, I., 2024. Nitrogen atmospheric deposition in a high-altitude Alpine environment: a chemical and isotopic approach to investigate the influence from anthropized areas. Atmos. Environ. 328, 120513. https://doi.org/10.1016/j.atmosenv.2024.120513.

Bargagli, R., 2016. Moss and lichen biomonitoring of atmospheric mercury: a review. Sci. Total Environ. 572, 216–231. https://doi.org/10.1016/j.scitotenv.2016.07.202.

Bargagli, R., Brown, D.H., Nelli, L., 1995. Metal biomonitoring with mosses: procedures for correcting for soil contamination. Environ. Pollut. 89, 169–175. https://doi.org/10.1016/0269-7491(94)00055-I.

Bargagli, R., Monaci, F., Borghini, F., Bravi, F., Agnorelli, C., 2002. Mosses and lichens as biomonitors of trace metals. A comparison study on *Hypnum cupressiforme* and *Parmelia* caperata in a former mining district in Italy. Environ. Pollut. 116, 279–287. https://doi.org/10.1016/S0269-7491(01)00125-7.

Barre, J.P.G., Deletraz, G., Sola-Larrañaga, C., Santamaria, J.M., Bérail, S., Donard, O.F. X., Amouroux, D., 2018. Multi-element isotopic signature (C, N, Pb, Hg) in epiphytic lichens to discriminate atmospheric contamination as a function of land-use characteristics (Pyrénées-Atlantiques, SW France). Environ. Pollut. 243, 961–971. https://doi.org/10.1016/j.envpol.2018.09.003.

Boltersdorf, S.H., Pesch, R., Werner, W., 2014. Comparative use of lichens, mosses and tree bark to evaluate nitrogen deposition in Germany. Environ. Pollut. 189, 43–53. https://doi.org/10.1016/j.envpol.2014.02.017.

Bragazza, L., Limpens, J., Gerdol, R., Grosvernier, P., Hájek, M., Hájek, T., Hajkova, P., Hansen, I., Iacumin, P., Kutnar, L., Rydin, H., Tahvanainen, T., 2005. Nitrogen concentration and δ^{15} N signature of ombrotrophic *Sphagnum* mosses at different N deposition levels in Europe. Glob. Change Biol. 11, 106–114. https://doi.org/10.1111/j.1365-2486.2004.00886.x.

Bramley-Alves, J., Wanek, W., French, K., Robinson, S.A., 2015. Moss δ^{13} C: an accurate proxy for past water environments in polar regions. Glob. Change Biol. 21, 2454–2464. https://doi.org/10.1111/gcb.12848.

Cai, X., Yuan, W., Zhang, Q., Luo, K., Xu, Y., Zhang, G., Wu, F., Jia, L., Sun, M., Liu, N., Lin, C.-J., Wang, X., Feng, X., 2024. Quantifying altitudinal mercury accumulation in biomonitors along Himalayan valleys using mercury isotopes. Environ. Sci. Technol. 58, 22183–22193. https://doi.org/10.1021/acs.est.4c10224.

Ciężka, M., Modelska, M., Górka, M., Trojanowska-Olichwer, A., Widory, D., 2016. Chemical and isotopic interpretation of major ion compositions from precipitation: a one-year temporal monitoring study in Wrocław, SW Poland. J. Atmos. Chem. 73, 61–80. https://doi.org/10.1007/s10874-015-9316-2.

Dawson, T.E., Mambelli, S., Plamboeck, A.H., Templer, P.H., Tu, K.P., 2002. Stable isotopes in plant ecology. Annu. Rev. Ecol. Syst. 33, 507–559. https://doi.org/10.1146/annurev.ecolsys.33.020602.095451.

Díaz-Álvarez, E.A., Lindig-Cisneros, R., De La Barrera, E., 2018. Biomonitors of atmospheric nitrogen deposition: potential uses and limitations. Conserv. Physiol. 6. https://doi.org/10.1093/conphys/coy011.

Deane-Coe, K.K., Mauritz, M., Celis, G., Salmon, V., Crummer, K.G., Natali, S.M., Schuur, E.A.G., 2015. Experimental warming alters productivity and isotopic signatures of tundra mosses. Ecosystems 18, 1070–1082. https://doi.org/10.1007/s10021-015-9884-7.

Donovan, M., Norman, A.-L., Reid, M.L., 2022. Local vehicles add nitrogen to moss biomonitors in a low-traffic protected wilderness area as revealed by a long-term isotope study. J. Nat. Conserv. 70, 126292. https://doi.org/10.1016/j.jnc.2022.126292.

Du, C., Guo, Q., Wu, P., Yi, Z., Wei, R., Dong, X., Zerizghi, T., Wang, Z., Zhang, J., 2024. Estimating atmospheric nitrogen deposition within a large river basin using moss nitrogen and isotope signatures. Chemosphere 347, 140617. https://doi.org/10.1016/j.chemosphere.2023.140617.

Du, C., Guo, Q., Zhang, J., 2022. A review on moss nitrogen and isotope signatures evidence for atmospheric nitrogen deposition. Sci. Total Environ. 806, 150765. https://doi.org/10.1016/j.scitotenv.2021.150765.

Felix, J.D., Avery, G.B., Mead, R.N., Kieber, R.J., Willey, J.D., 2016. Nitrogen content and isotopic composition of Spanish moss (*Tillandsia usneoides* L.): reactive nitrogen variations and source implications across an urban coastal air shed. Environ. Process. 3, 711–722. https://doi.org/10.1007/s40710-016-0195-6.

Foan, L., Leblond, S., Thöni, L., Raynaud, C., Santamaría, J.M., Sebilo, M., Simon, V., 2014. Spatial distribution of PAH concentrations and stable isotope signatures ($\delta^{13}C$, $\delta^{15}N$) in mosses from three European areas - characterization by multivariate analysis. Environ. Pollut. 184, 113–122. https://doi.org/10.1016/j.envpol.2013.08.006.

Fowler, D., Coyle, M., Skiba, U., Sutton, M.A., Cape, J.N., Reis, S., Sheppard, L.J., Jenkins, A., Grizzetti, B., Galloway, J.N., Vitousek, P., Leach, A., Bouwman, A.F., Butterbach-Bahl, K., Dentener, F., Stevenson, D., Amann, M., Voss, M., 2013. The global nitrogen cycle in the twenty-first century. Phil. Trans. R. Soc. B 368, 20130164. https://doi.org/10.1098/rstb.2013.0164.

Galloway, J.N., Aber, J.D., Erisman, J.W., Seitzinger, S.P., Howarth, R.W., Cowling, E.B., Cosby, B.J., 2003. The nitrogen cascade. Bioscience 53 (2), 341. https://doi.org/10.1641/0006-3568(2003)053%255B0341:TNC%255D2.0.CO.

Galloway, J.N., Townsend, A.R., Erisman, J.W., Bekunda, M., Cai, Z., Freney, J.R., Martinelli, L.A., Seitzinger, S.P., Sutton, M.A., 2008. Transformation of the nitrogen cycle: recent trends, questions, and potential solutions. Science 320, 889–892. https://doi.org/10.1126/science.1136674.

Galloway, J.N., Cowling, E.B., 2021. Reflections on 200 years of nitrogen, 20 years later. Ambio 50, 745–749. https://doi.org/10.1007/s13280-020-01464-z.

Gelman, A., Rubin, D.B., 1992. Inference from Iterative simulation using multiple sequences. Statist. Sci. 7. https://doi.org/10.1214/ss/1177011136.

Harmens, H., Norris, D.A., Cooper, D.M., Mills, G., Steinnes, E., Kubin, E., Thöni, L., Aboal, J.R., Alber, R., Carballeira, A., Coşkun, M., De Temmerman, L., Frolova, M., González-Miqueo, L., Jeran, Z., Leblond, S., Liiv, S., Maňkovská, B., Pesch, R., Poikolainen, J., Rühling, Å., Santamaria, J.M., Simonèiè, P., Schröder, W., Suchara, I., Yurukova, L., Zechmeister, H.G., 2011. Nitrogen concentrations in mosses indicate the spatial distribution of atmospheric nitrogen deposition in Europe. Environ. Pollut. 159, 2852–2860. https://doi.org/10.1016/j.envpol.2011.04.041.

Harmens, H., Norris, D.A., Sharps, K., Mills, G., Alber, R., Aleksiayenak, Y., Blum, O., Cucu-Man, S.-M., Dam, M., De Temmerman, L., Ene, A., Fernández, J.A., Martinez-Abaigar, J., Frontasyeva, M., Godzik, B., Jeran, Z., Lazo, P., Leblond, S., Liiv, S., Magnússon, S.H., Maňkovská, B., Karlsson, G.P., Piispanen, J., Poikolainen, J., Santamaria, J.M., Skudnik, M., Spiric, Z., Stafilov, T., Steinnes, E., Stihi, C., Suchara, I., Thöni, L., Todoran, R., Yurukova, L., Zechmeister, H.G., 2015. Heavy metal and nitrogen concentrations in mosses are declining across Europe whilst some "hotspots" remain in 2010. Environ. Pollut. 200, 93–104. https://doi.org/10.1016/j.envpol.2015.01.036.

Harmens, H., Schnyder, E., Thöni, L., Cooper, D.M., Mills, G., Leblond, S., Mohr, K., Poikolainen, J., Santamaria, J., Skudnik, M., Zechmeister, H.G., Lindroos, A.-J., Hanus-Illnar, A., 2014. Relationship between site-specific nitrogen concentrations in mosses and measured wet bulk atmospheric nitrogen deposition across Europe. Environ. Pollut. 194, 50–59. https://doi.org/10.1016/j.envpol.2014.07.016.

Heaton, T.H.E., Spiro, B., Robertson, S.M.C., 1997. Potential canopy influences on the isotopic composition of nitrogen and sulphur in atmospheric deposition. Oecologia 109, 600–607. https://doi.org/10.1007/s004420050122.

ICP Vegetation, 2020. Heavy Metals, Nitrogen and Pops in European Mosses: 2020 Survey. ICP Vegetation Programme Coordination Centre, Centre for Ecology & Hydrology, Bangor, UK. Monitoring Manual 27. Available at: https://icpvegetation.ceh.ac.uk/sites/default/files/ICP%20Vegetation%20moss%20monitoring%20manual%202020.pdf. (Accessed 19 April 2026).

Izquieta-Rojano, S., Elustondo, D., Ederra, A., Lasheras, E., Santamaría, C., Santamaría, J.M., 2016. *Pleurochaete squarrosa* (Brid.) lindb. as an alternative moss species for biomonitoring surveys of heavy metal, nitrogen deposition and $\delta^{15}N$ signatures in a Mediterranean area. Ecol. Indic. 60, 1221–1228. https://doi.org/10.1016/j.ecolind.2015.09.023.

Izquieta-Rojano, S., Morera-Gómez, Y., Elustondo, D., Lasheras, E., Santamaría, C., Torrens-Baile, J., Alber, R., Barandovski, L., Coşkun, M., Coskun, M., Danielsson, H., De Temmerman, L., Harmens, H., Jeran, Z., Leblond, S., Martínez-Abaigar, J., Núñez-Olivera, E., Pesch, R., Pihl Karlsson, G., Piispanen, J., Soja, G., Spiric, Z., Stafilov, T., Thöni, L., Santamaría, J.M., 2025. Spatial distribution and isotopic signatures of N and C in mosses across Europe. Sci. Total Environ. 958, 178043. https://doi.org/10.1016/j.scitotenv.2024.178043.

Jafarova, M., Aherne, J., Renzi, M., Anselmi, S., Zinicovscaia, I., Yushin, N., Bonini, I., Loppi, S., 2025. Is moss still a reliable biomonitor of nitrogen and sulfur deposition after decades of emissions reductions? Plants 14, 1114. https://doi.org/10.3390/plants14071114.

Lattanzi, P., 1999. Epithermal precious metal deposits of Italy - an overview. Miner. Deposita 34, 630–638. https://doi.org/10.1007/s001260050224.

Legnaro Diamanti, M., Fedeli, R., Alnaqshabandi, R., Fiaschi, T., Tremori, G., Angiolini, C., Loppi, S., 2026. Biochemical differences between *Hypnum cupressiforme* and *Pseudoscleropodium purum*. A case study from across remote sites in Tuscany (central Italy). Plant Biosyst. 160. https://doi.org/10.1007/s44473-026-00112-w.

Li, X., Wang, X., Zhang, H., Lu, Z., 2023. Mosses and lichens enhance atmospheric elemental mercury deposition in a subtropical montane forest. Environ. Chem. 20, 105–113. https://doi.org/10.1071/EN22124.

Lovreškov, L., Limić, I., Butorac, L., Jakovljević, T., 2021. Nitrogen deposition in different Mediterranean forest types along the eastern Adriatic coast. SEEFOR 12, 115–122. https://doi.org/10.15177/seefor.21-15.

McLagan, D.S., Monaci, F., Huang, H., Lei, Y.D., Mitchell, C.P.J., Wania, F., 2019. Characterization and quantification of atmospheric mercury sources using passive air samplers. J. Geophys. Res. Atmos. 124, 2351–2362. https://doi.org/10.1029/2018JD029373.

Monaci, F., Ancora, S., Paoli, L., Loppi, S., Franzaring, J., 2023. Air quality in post-mining towns: tracking potentially toxic elements using tree leaves. Environ. Geochem. Health 45, 843–859. https://doi.org/10.1007/s10653-022-01252-6.

Monaci, F., Baroni, D., 2025. Spatial distribution and ecological risk of potentially toxic elements in peri-urban soils of a historically industrialised area. Environ. Monit. Assess. 197, 948. https://doi.org/10.1007/s10661-025-14389-5.

Obrist, D., Roy, E.M., Harrison, J.L., Kwong, C.F., Munger, J.W., Moosmueller, H., Romero, C.D., Sun, S., Zhou, J., Commane, R., 2021. Previously unaccounted atmospheric mercury deposition in a midlatitude deciduous forest. Proc. Natl. Acad. Sci. U. S. A. 118, e2105477118. https://doi.org/10.1073/pnas.2105477118.

Oenema, O., Bleeker, A., Braathen, N.A., Budňáková, M., Bull, K., Čermák, P., Geupel, M., Hicks, K., Hoft, R., Kozlova, N., Leip, A., Spranger, T., Valli, L., Velthof, G., Winiwarter, W., 2011. Nitrogen in current European policies. In: Sutton, M.A., Howard, C.M., Erisman, J.W., Billen, G., Bleeker, A., Grennfelt, P., Van Grinsven, H., Grizzetti, B. (Eds.), The European Nitrogen Assessment. Cambridge University Press, Cambridge, pp. 62–81. https://doi.org/10.1017/CBO9780511976988.007.

Oishi, Y., 2019. Moss as an indicator of transboundary atmospheric nitrogen pollution in an alpine ecosystem. Atmos. Environ. 208, 158–166. https://doi.org/10.1016/j.atmosenv.2019.04.005.

Oishi, Y., Hiura, T., 2017. Bryophytes as bioindicators of the atmospheric environment in urban-forest landscapes. Landsc. Urban Plan. 167, 348–355. https://doi.org/10.1016/j.landurbplan.2017.07.010.

Pasquetti, F., Vaselli, O., Zanchetta, G., Nisi, B., Lezzerini, M., Bini, M., Mele, D., 2020. Sedimentological, mineralogical and geochemical features of late Quaternary sediment profiles from the Southern Tuscany Hg mercury district (Italy): evidence for the presence of pre-industrial mercury and arsenic concentrations. Water 12, 1998. https://doi.org/10.3390/w12071998.

Petix, M.I., Bell, M.D., Williams, D.G., Evans, R.D., 2024. Utilizing $\delta^{15}N$ of biomonitors to assess N emission sources and deposition chemistry? Ecol. Indic. 169, 112866. https://doi.org/10.1016/j.ecolind.2024.112866.

Phillips, D.L., Inger, R., Bearhop, S., Jackson, A.L., Moore, J.W., Parnell, A.C., Semmens, B.X., Ward, E.J., 2014. Best practices for use of stable isotope mixing models in food-web studies. Can. J. Zool. 92, 823–835. https://doi.org/10.1139/cjz-2014-0127.

Pinho, P., Barros, C., Augusto, S., Pereira, M.J., Máguas, C., Branquinho, C., 2017. Using nitrogen concentration and isotopic composition in lichens to spatially assess the relative contribution of atmospheric nitrogen sources in complex landscapes. Environ. Pollut. 230, 632–638. https://doi.org/10.1016/j.envpol.2017.06.102.

Poggiali, F., Buonincontri, M.P., D'Auria, A., Volante, N., Di Pasquale, G., 2017. Wood selection for firesetting: first data from the Neolithic cinnabar mine of Spaccasasso (South Tuscany, Italy). Quat. Int. 458, 134–140. https://doi.org/10.1016/j.quaint.2017.06.028.

Protano, G., Bianchi, S., De Santis, M., Di Lella, L.A., Nannoni, F., Salleolini, M., 2023. New geochemical data for defining origin and distribution of mercury in groundwater of a coastal area in southern Tuscany (Italy). Environ. Sci. Pollut. Res. 30, 50920–50937. https://doi.org/10.1007/s11356-023-25897-7.

R Core Team, 2025. R: a Language and Environment for Statistical Computing. R Foundation for Statistical Computing, Vienna, Austria.

Reimann, C., Filzmoser, P., Garrett, R.G., 2005. Background and threshold: critical comparison of methods of determination. Sci. Total Environ. 346, 1–16. https://doi.org/10.1016/j.scitotenv.2004.11.023.

Schröder, W., Nickel, S., Dreyer, A., Völksen, B., 2023. Accumulation of atmospheric metals and nitrogen deposition in mosses: temporal development between 1990 and 2020, comparison with emission data and tree canopy drip effects. Pollutants 3, 89–101. https://doi.org/10.3390/pollutants3010008.

Scott, D.L., Bradley, R.L., Bellenger, J.-P., Houle, D., Gundale, M.J., Rousk, K., DeLuca, T. H., 2018. Anthropogenic deposition of heavy metals and phosphorus may reduce biological N_2 fixation in boreal forest mosses. Sci. Total Environ. 630, 203–210. https://doi.org/10.1016/j.scitotenv.2018.02.192.

Seinfeld, J.H., Pandis, S.N., 2016. Atmospheric Chemistry and Physics: from Air Pollution to Climate Change, third ed. Wiley, Hoboken, NJ.

Shao, J., Liu, C., Zhang, Q., Fu, J., Yang, R., Shi, J., Cai, Y., Jiang, G., 2017. Characterization and speciation of mercury in mosses and lichens from the high-altitude Tibetan Plateau. Environ. Geochem. Health 39, 475–482. https://doi.org/10.1007/s10653-016-9828-y.

Skrzypek, G., Kałużny, A., Wojtuń, B., Jędrysek, M.-O., 2007. The carbon stable isotopic composition of mosses: a record of temperature variation. Org. Geochem. 38, 1770–1781. https://doi.org/10.1016/j.orggeochem.2007.05.002.

Solga, A., Eichert, T., Frahm, J.-P., 2006. Historical alteration in the nitrogen concentration and ^{15}N natural abundance of mosses in Germany: Indicationifor regionally varying changes in atmospheric nitrogen deposition within the last 140 years. Atmos. Environ. 40, 8044–8055. https://doi.org/10.1016/j.atmosenv.2006.03.024.

Sonke, J.E., Angot, H., Zhang, Y., Poulain, A., Björn, E., Schartup, A., 2023. Global change effects on biogeochemical mercury cycling. Ambio 52, 853–876. https://doi.org/10.1007/s13280-023-01855-y.

Steinnes, E., Rühling, Å., Lippo, H., Mäkinen, A., 1997. Reference materials for large-scale metal deposition surveys. Accredit Qual. Assur. 2, 243–249. https://doi.org/10.1007/s007690050141.

Stock, B.C., Jackson, A.L., Ward, E.J., Parnell, A.C., Phillips, D.L., Semmens, B.X., 2018. Analyzing mixing systems using a new generation of Bayesian tracer mixing models. PeerJ 6, e5096. https://doi.org/10.7717/peerj.5096.

Stock, B.C., Semmens, B.X., 2016. Unifying error structures in commonly used biotracer mixing models. Ecology 97, 2562–2569. https://doi.org/10.1002/ecy.1517.

Sutton, M.A., Fowler, D., Moncrieff, J.B., 1993. The exchange of atmospheric ammonia with vegetated surfaces. I: unfertilized vegetation. Q. J. R. Meteorol. Soc. 119, 1023–1045. https://doi.org/10.1002/qj.49711951309.

Vannini, A., Tedesco, R., Loppi, S., Di Cecco, V., Di Martino, L., Nascimbene, J., Dallo, F., Barbante, C., 2021. Lichens as monitors of the atmospheric deposition of potentially toxic elements in high elevation Mediterranean ecosystems. Sci. Total Environ. 798, 149369. https://doi.org/10.1016/j.scitotenv.2021.149369.

Xiao, H.-Y., Tang, C.-G., Xiao, H.-W., Liu, X.-Y., Liu, C.-Q., 2010. Stable sulphur and nitrogen isotopes of the moss *Haplocladium microphyllum* at urban, rural and forested sites. Atmos. Environ. 44, 4312–4317. https://doi.org/10.1016/j.atmosenv.2010.05.023.

Xu, Y., Xiao, H., Wu, D., 2019. Traffic-related dustfall and NO_x, but not NH_3, seriously affect nitrogen isotopic compositions in soil and plant tissues near the roadside. Environ. Pollut. 249, 655–665. https://doi.org/10.1016/j.envpol.2019.03.074.

Xu, Y., Yuan, W., Ma, W., Liu, N., Jia, L., Sun, M., Zhang, H., Lin, C.-J., Wang, X., Feng, X., 2026. Low biomass, high impact: mosses and lichens dominate mercury sequestration in the alpine forest. Environ. Sci. Technol. https://doi.org/10.1021/acs.est.6c01878 acs.est.6c01878.

Zechmeister, H.G., Richter, A., Smidt, S., Hohenwallner, D., Roder, I., Maringer, S., Wanek, W., 2008. Total nitrogen content and $\delta^{15}N$ signatures in moss tissue: Indicativeivalue for nitrogen deposition patterns and source allocation on a nationwide scale. Environ. Sci. Technol. 42, 8661–8667. https://doi.org/10.1021/es801865d.

Zeng, S., Li, X., Yang, L., Wang, D., 2023. Understanding heavy metal distribution in timberline vegetations: a case from the Gongga Mountain, eastern Tibetan Plateau. Sci. Total Environ. 874, 162523. https://doi.org/10.1016/j.scitotenv.2023.162523.

Zhao, J., Zhang, Z., Zhu, G., Zheng, N., Xiao, Hongwei, Tian, J., Zhou, Y., Guan, H., Xiao, H., 2019. The $\delta^{15}N$ values of epilithic mosses indicating the changes of nitrogen sources in Guiyang (SW China) from 2006 to 2016–2017. Sci. Total Environ. 696, 133988. https://doi.org/10.1016/j.scitotenv.2019.133988.

Zhou, J., Obrist, D., Dastoor, A., Jiskra, M., Ryjkov, A., 2021. Vegetation uptake of mercury and impacts on global cycling. Nat. Rev. Earth Environ. 2, 269–284. https://doi.org/10.1038/s43017-021-00146-y.